

## Preparation and characterization of ZnO nanoparticles incorporated by mechanical milling into cellulose for electrical insulator applications

A. Guesmi<sup>a,b,c</sup>, W. Abdulfattah<sup>a</sup>, M. ben Ticha<sup>d</sup>, F. K. Alghathami<sup>a</sup>, K. Aouadi<sup>c,e</sup>, J. El Ghoul<sup>f</sup>, A. Houas<sup>g</sup>, N. Ben Hamadi<sup>a,c,\*</sup>

<sup>a</sup> Chemistry Department, College of Science, IMSIU (Imam Mohammad Ibn Saud Islamic University), P.O. Box 5701, Riyadh 11432, Saudi Arabia.

<sup>b</sup> Textile Engineering Laboratory, Higher Institute of Technological Studies of Ksar, University of Monastir, Hellal, Tunisia.

<sup>c</sup> Laboratory of Heterocyclic Chemistry, Natural Products and Reactivity (LR11ES39), Faculty of Science of Monastir, University of Monastir, Avenue of Environment, 5019 Monastir, Tunisia.

<sup>d</sup> Department of Early Childhood, University College of Turabah, Taif University, P.O. Box 11099, Taif 21944, Saudi Arabia.

<sup>e</sup> Department of Chemistry, College of Science, Qassim University, Buraidah 51452, Saudi Arabia.

<sup>f</sup> Department of Physics, College of Sciences, Imam Mohammad Ibn Saud Islamic University (IMSIU), Riyadh 11623, Saudi Arabia

<sup>g</sup> Laboratoire de Catalyse et Matériaux pour l'Environnement et les Procédés LRCMEP (LR19ES08) Faculté des Sciences de Gabès/ Université de Gabès - Campus Universitaire 6072 Gabès- Tunisia.

In this work, a novel composite material based on ZnO nanoparticles incorporated into cellulose polymers has been designed and prepared. For this purpose, the *ex-situ* prepared ZnO nanoparticles were dispersed into cellulose using mechanical milling. The effect of the percentage of ZnO nanoparticles doping into the prepared composite was studied. Dielectric properties of composite, as influenced by the compaction density, the level of ZnO nanoparticles doping into cellulose, and the temperature, were characterized using a liquid test fixture, a precision inductance capacitance and resistance meter at a radio frequency ranging from 5 to 30 MHz. It has been shown that  $\epsilon'$  and  $\epsilon''$  respectively correspondent to the dielectric constant and the loss factor of composite were affected by level of ZnO nanoparticles, compaction density and temperature of the samples. Both  $\epsilon'$  and  $\epsilon''$  increased with increasing the temperature and the level of ZnO nanoparticles, but decreased with increasing the frequency.

(Received January 25, 2022; Accepted May 4, 2022)

**Keywords:** Cellulose, ZnO nanoparticles, Electrical properties, Mechanical milling, Radio frequency

### 1. Introduction

Cellulose, one of the worlds's the majority rich usual and sustainable biopolymers assets, is future reaching in various types of biomasses, such plants, trees, microorganisms and tunicate.

One of the basic uses for cellulose incorporates electrical covers, broadly utilized in oil-filled force transformers and paper-protected force links.<sup>1-4</sup>

Improving the quality of daily life has always been one of the major concerns of the man. It is in this context that the perpetual search for new and better materials is part of adapted to the requirements of the time. Currently, the cellulose is required for many applications to such an extent that we could not imagine the lives of all the days without these! These polymeric materials

---

\* Corresponding author: nabenhamadi@imamu.edu.sa  
<https://doi.org/10.15251/DJNB.2022.172.579>

are used in areas of daily life as diverse as automotive, packaging, building and other sectors cosmetics but also in more specific sectors: biomedical, pharmaceutical, optoelectronics or aeronautics. Some researchers have studied the dielectric properties of modified cellulose by on many factors.<sup>5-8</sup> In recent years, we have seen prompt development of materials appropriate in the fabrication of smart garments.<sup>9</sup> These kinds of garments often use a different type of transmission line frequently made of conventional metal wires.

The objective of this work was to describe the dielectric character of zinc oxide nanoparticles incorporated into cellulose (ZnO@cellulose).

## **2. Materials and methods**

### **2.1. Chemicals**

Zinc oxide, ReagentPlus®, powder, <5 µm particle size, cellulose 99.9%, were purchase from Sigma-Aldrich.

### **2.2. Instrumentation**

#### **2.2.1. Ball milling**

Planetary Micro Mill Pulverisette 7 was utilized for ball milling in this work. Great line with 45 milliliter tempers steel vials and 10-millimeter temper steel granulation balls.

### **2.3. X-ray diffractometry**

The X-ray diffraction examination was abandoned with a Schimadzu ( $\theta - 2\theta$ ) diffractometer (Shimadzu apparatus). The composite samples were mounted in the sample holder. All samples were tested in triplicate to obtain demanding presentation results and the average was considered.

### **2.4. Transmission Electron Microscope (TEM) and Scanning electron microscope (SEM) and Energy Dispersive X-Ray (EDX)**

JEOL JEM-1011 (TEM) was used to the morphology studies. SEM analysis was performed using Jeol Model 6360 LVSEM, USA. The distribution of particle-size was calculated using SMiLe View Ver. 2. 728, which was developed by Jeol Ltd.

### **2.5. Methods**

#### **2.5.1. Preparation ZnOPs**

ZnO aerogel nanoparticles were prepared by dissolving 2 g of zinc acetate dihydrate ( $\text{Zn}(\text{CH}_3\text{COO})_2 \cdot 2\text{H}_2\text{O}$ ) in 14 mL of methanol, purchased from Sigma-Aldrich. After 30 min magnetic stirring at room temperature, the solution was placed in an autoclave and dried under supercritical conditions in ethyl alcohol (EtOH).<sup>10</sup> The obtained powders were annealed at 500 °C in air for two hours.

### **2.6. Incorporation of ZnONPs into cellulose using ball milling**

In the first step, 1.5 g of cellulose was located in hardened steel ball grinding flasks with 8.61 g of 10 mm hardened steel balls (4 balls). The bottles were closed and then placed in a Micro Mill apparatus, which is set to 10 hours and 650 rpm. In the second step, ZnO nanoparticles (2, 4, 6, 8, 10%) with a fixed molar of crushed cellulose obtained in the first step were added to 4.30 g of two balls into the vial. The bottles were closed and placed in the planetary micro-mill, which is then set to 650 rpm. ZnO@cellulose were obtained after 7 hours of grinding.

### **2.7. Measurement of dielectric properties of ZnO@cellulose**

The parallel capacitance ( $C_p$ ) and resistance ( $R_p$ ) of the ZnO@cellulose were measured using a liquid test fixture (16452, Agilent Technologies, Palo Alto, CA) and an inductance Capacitance and Resistance (LCR) meter (4285A, Agilent Technologies, Palo Alto, CA).<sup>11</sup> Before each test, the text fixture has been, at first, subjected to an abundant washing treatment using distilled water and then dried before being calibrated.

Samples of 2g of ZnO@cellulose were used in the measurement of the dielectric properties.

The test fixture containing the sample, has been firmly closed. The test fixture connected by its BNC connector to the LCR meter, was retained into a temperature chamber and subjected to heating treatment during 50 min to obtain temperatures varying with an interval of 10 °C from 20 to 80 °C. To detect the temperature variation of the tested sample during heating, a fiber optic temperature sensor coupled to a data logger was used. At each temperature, the Cp and Rp of the ZnO@cellulose were measured, using the LCR meter, with varying frequency in an interval ranged from 1 to 30 MHz.

$\epsilon'$  and  $\epsilon''$  have been calculated referring to the measured values of Cp and Rp using the following equations:<sup>12</sup>

$$\epsilon' = \frac{DCp}{A\epsilon_0}$$

D: The gap (m) between electrodes of the test fixture,

Cp: The parallel capacitance (F),

Rp: The resistance (U),

F: The frequency (Hz),

$\epsilon'$ : The permittivity of vacuum ( $8.854 \times 10^{-12}$  F m<sup>-1</sup>)

A: The electrode area (m<sup>2</sup>).

Samples of ZnO@cellulose have been prepared at various weight (varying from 0.5 to 3 g) in order to evaluate the effect of compaction density of ZnO@cellulose on the measured dielectric properties. The prepared samples were fixed using a spacer in the test fixture at a depth of 1.5 mm. Samples were spread homogeneously by tapping (10 times) and then compressed by the top of the test fixture to squeeze the air out from inside of the powder. To avoid the discharge of air and moisture from the test fixture, it was firmly closed with sealing its inlet and outlet from inside. The compaction density (g/mL) was calculated by dividing the weight of the sample by its volume,

Noting that the volume equals to  $\pi \cdot (0.01 \text{ m})^2 \cdot (0.0015 \text{ m}) = 4.71 \cdot 10^{-7} \text{ m}^3$ , where 0.01 m corresponds to the radius of the inside bottom of the fixture and 0.0015 m corresponds to its depth.

### 2.8. Measurement of power penetration depth (dp)

The estimation of the heating uniformity and the design of an RF heating system are imperatively related to the penetration depth parameter. This latter could be expressed as follow:<sup>13</sup>

$$\epsilon'' = \frac{D}{2\pi f R_p \epsilon_0 A}$$

where:

c: the speed of light in air ( $3 \times 10^8$  m s<sup>-1</sup>),

$\tan \delta$  is defined as ( $\epsilon''/\epsilon'$ ).

$\epsilon'$  and  $\epsilon''$  values served to calculate the power penetration depth dp (m) of RF in the ZnO@cellulose samples with different compaction densities at given frequencies (13.56 and 27.12 MHz) and temperatures values (ranging from 20 to 80 °C).

### 2.9. Determination of dielectric character of ZnO@cellulose

The dielectric character of ZnO@cellulose was account by calculating the resistance and the parallel capacity (Cp) with the power and resistance inductance meter (LCR) and the liquid test system.<sup>14</sup> The system was calibrated previous to the measurements. For each measure, 2 g of ZnO@cellulose were located in the test machine, which was then strongly closed.

### 3. Results and discussion

#### 3.1. Preparation of ZnOPs

TEM micrograph of ZnO nanoparticles is illustrated in Fig.1. The morphology of nanoparticles shown obvious spherical shape with diameters ranging from 20 nm to 50 nm.

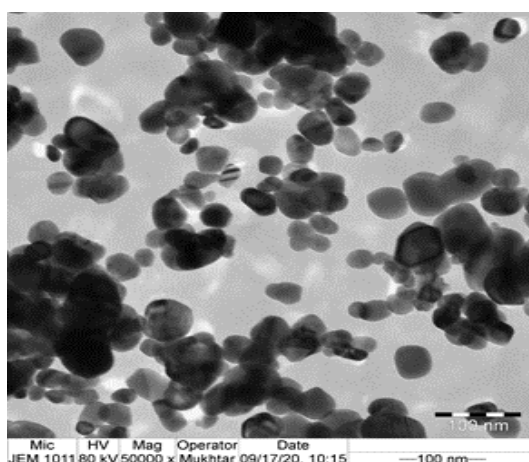
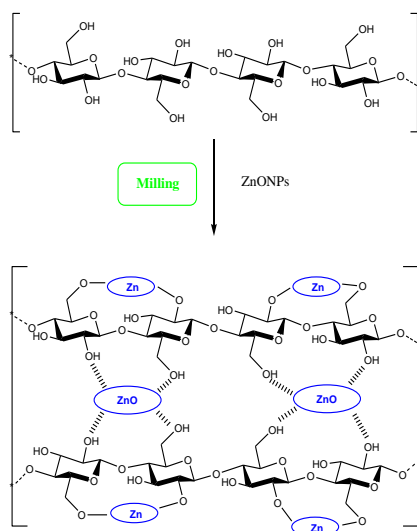


Fig. 1. TEM image of ZnO nanoparticles.

#### 3.2. Preparation of composite cellulose@ZnONPs

Our route to the target composite is summarized in Scheme 1. The reaction of the cellulose with ZnO nanoparticles under elevated speed grinding (650 rpm) by vibration for 7 hours made it possible to obtain ZnO@cellulose. Natural cellulose has a nonwoven network with a big number of pores.<sup>15</sup> These pores facilitate the adsorption of ZnO nanoparticles in cellulose which should interact with electro-positive metallions.



Scheme 1. Synthesis of ZnO@cellulose by mechanical milling.

#### 3.3. The structure of the composite

Figure 2 show the diffraction patterns of cellulose (a), ZnO nanoparticles (b) and ZnO@cellulose (c). The two spectra (a and c) indicated three peaks at  $2\theta = 14.62^\circ$ ,  $16.29^\circ$  and  $22.48^\circ$  correspond to the cellulose (Figure 2-a).

A definitive widening of the line of peaks XRD confirmed the dimensions at the nanometric scale of the material obtained. Analysis of the XRD models, determined the peak intensity, position and width, full width at half of the maximum data.

The diffraction peaks situated at  $31.80^\circ$ ,  $34.54^\circ$ ,  $36.30^\circ$ ,  $47.61^\circ$ ,  $56.69^\circ$ ,  $62.93^\circ$ ,  $68.11^\circ$ , and  $69.19^\circ$  have been eagerly affirmed as hexagonal wurtzite phase of Zinc oxide<sup>16,17</sup> with lattice constants  $a=b=0.321$  nm and  $c=0.522$  nm,<sup>18</sup> and it also affirms that the prepared nanoparticle was pure product. The XRD does not include any peaks other than zinc oxide peaks (Figure 2-b). The diameter of prepared ZnO nanoparticle was measured by Debye-Scherrer equation and ranging from 20 nm to 50 nm.<sup>19</sup> Fig. 1c shows the diffraction peaks characteristic of the crystal structure of the ZnO and three peaks confirmed that the ZnO nanoparticles was incorporated by the cellulose.

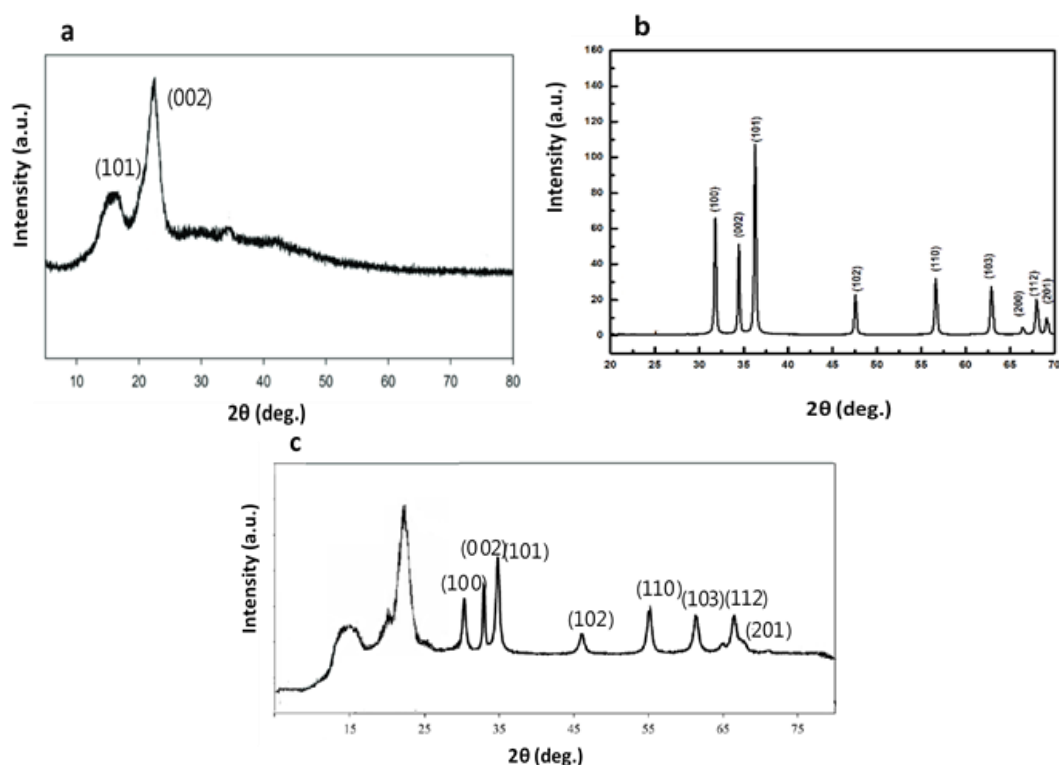


Fig. 2. XRD diffractogram of cellulose (a), ZnO nanoparticles (b) and cellulose@ZnONPs (c).

The image SEM of the cellulose powder (figure 3-a) confirmed a rough surface with some cracks and pores. The incorporation of ZnONP enhanced the compactness and the density of the film due to the reduction of the film of pores and cracks affirmed a strong affinity between ZnONP and cellulose (figure 3-b). ZnONPs dispersed individually and uniformly across the films with less agglomeration.

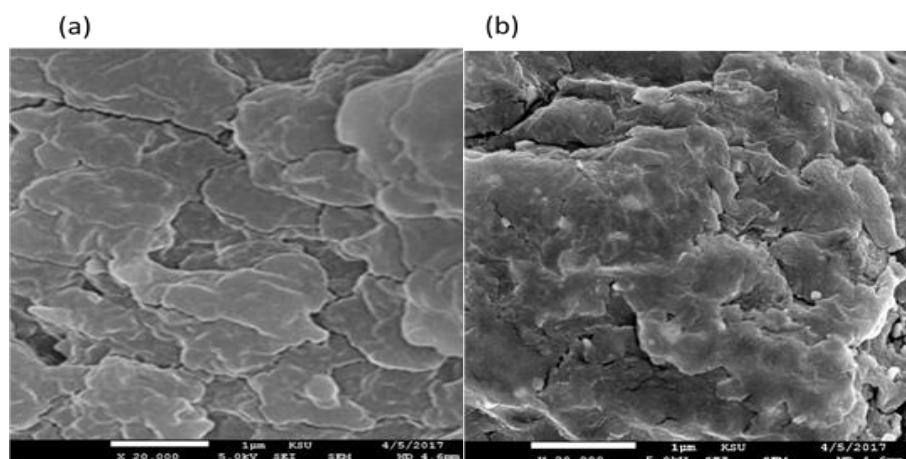


Fig. 3. Scanning electron microscopy images of cellulose powder (a) and composite (b).

An EDX analysis was carried out to study the elementary composition of the composite and to confirm the presence of ZnO nanoparticles in cellulose (Figure 4). The EDX spectra showed various intense peaks associated with the atoms of Zn, O and C for the composite.

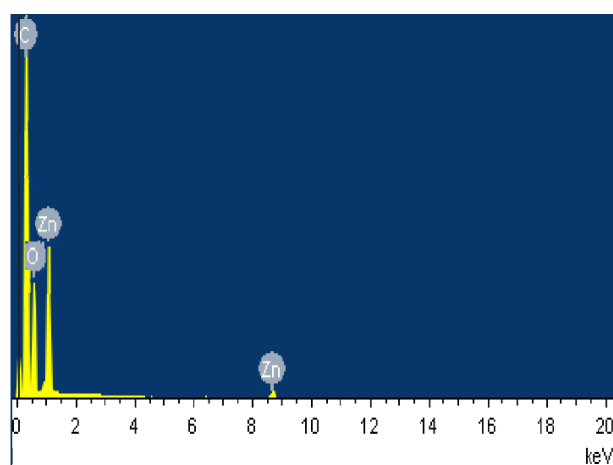


Fig. 4. EDX analysis of the composite.

### 3.4. Dielectric character of ZnO@cellulose at diverse frequencies

The dielectric characters of the composite at room temperature ( $25 \pm 2$  ° C) with a practical frequency are illustrated in Figure 5. It demonstrates that ZnO@cellulose has the diverse values of dielectric loss factor and dielectric constant. When the frequency increases from 5 to 30 MHz, the values of the dielectric loss factor and the dielectric constant decrease. The values of the dielectric constants follow the percentage order of ZnO = 10 > 8 > 6 > 4 > 2. These results affirm that the percentage of ZnO is one of the most significant parameters affect the dielectric character of ZnO@cellulose. The dielectric constant in ZnO@cellulose decrease with frequency, this result can be clarified by the modification in ion mobility and conduction of the composite.

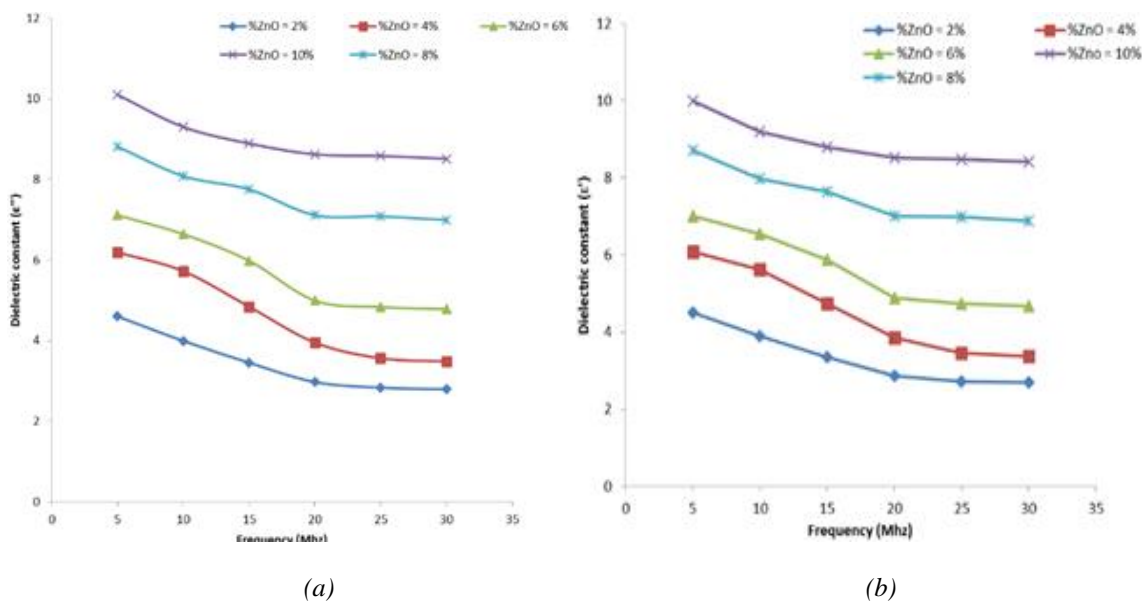


Fig. 5. The variation of the dielectric constant (a) and the loss factor (b) of cellulose@ZnONPs as a function of the frequency.

### 3.5. Variation of dielectric properties and penetration depth as a function of the compaction density

During packaging of ZnO@cellulose, the material can be subjected to a shaking and compression movement leading to increase the compaction density.

Table 1 and figure 6 summarize the variation of  $\epsilon'$  and  $\epsilon''$  values depending on the compaction density. As exposed, at a given frequency, both  $\epsilon'$  and  $\epsilon''$  increase in accordance with the increase of the compaction density till reaching a certain level, above it they started to decrease.

Table 1. Variation of the ZnO@cellulose dielectric properties values (mean  $\pm$  standard deviation of replicates) as a function of the compaction densities at  $25 \pm 3$  °C. The percentage of ZnO 10%.

	Compaction density (g/ml)	$\epsilon'$		$\epsilon''$		Penetration depth (m)	
		13.56 Mhz	27.12 Mhz	13.56 Mhz	27.12 Mhz	13.56 Mhz	27.12 Mhz
% ZnO = 10%	0.14	6.79 $\pm$ 0.31	6.46 $\pm$ 0.2	0.35 $\pm$ 0.04	0.18 $\pm$ 0.11	1.11 $\pm$ 0.08	0.66 $\pm$ 0.04
	0.29	6.92 $\pm$ 0.22	6.55 $\pm$ 0.42	0.39 $\pm$ 0.08	0.25 $\pm$ 0.05	1.09 $\pm$ 0.05	0.64 $\pm$ 0.03
	0.44	7.97 $\pm$ 0.15	7.57 $\pm$ 0.24	0.58 $\pm$ 0.05	0.37 $\pm$ 0.07	0.99 $\pm$ 0.16	0.55 $\pm$ 0.08
	0.58	8.23 $\pm$ 0.32	7.78 $\pm$ 0.14	0.66 $\pm$ 0.12	0.41 $\pm$ 0.09	0.95 $\pm$ 0.22	0.5 $\pm$ 0.09
	0.73	8.56 $\pm$ 0.04	8.01 $\pm$ 0.21	0.72 $\pm$ 0.15	0.43 $\pm$ 0.04	0.94 $\pm$ 0.17	0.57 $\pm$ 0.1
	0.88	7.22 $\pm$ 0.09	7.56 $\pm$ 0.18	0.61 $\pm$ 0.13	0.29 $\pm$ 0.05	1.07 $\pm$ 0.12	0.67 $\pm$ 0.11

It also to note that the penetration depths in ZnO@cellulose augmented till a certain value and above this level it decreased, parallel to the variation in dielectric constant and dielectric loss factor. At a frequency value of 27.12 MHz and a compaction density about 0.88 g/mL, the penetration depths of ZnO@cellulose ranged from 0.88 and 0.5 m.

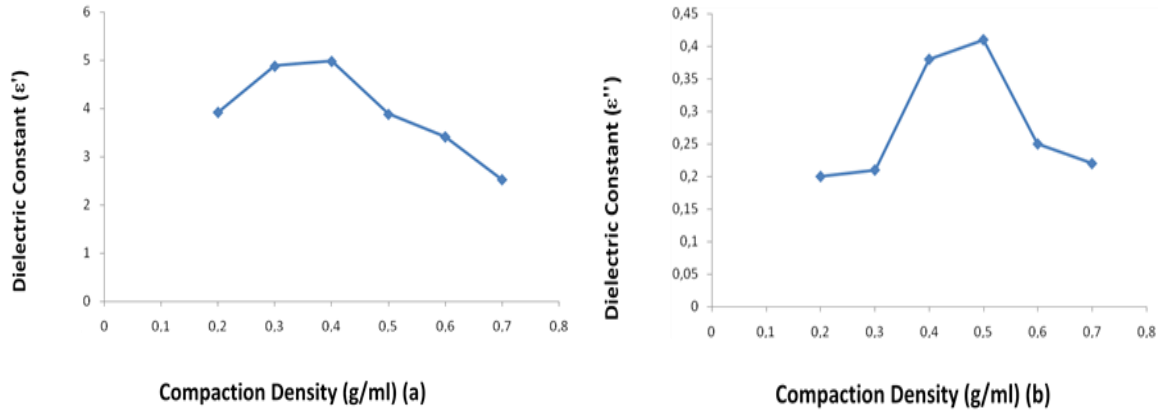


Fig. 6. Variation of dielectric constant (a) and loss factor (b) of ZnO@cellulose as a function of the compaction density at 27.12 MHz.

### 3.6. Effect of moisture and temperature on dielectric properties

A study on the effect of moisture and temperature on the dielectric properties have been also conducted. Results are summarized in figure 7. A fast variation in dielectric properties was observed especially at high moisture content (14.9%). For the 14.9% moisture sample, in parallel to the increase of the temperature from 20 to 80 °C, the dielectric constant augmented from 5.1 to 25.4 and the loss factor augmented from 1.1 to 8.06 at 27.12 MHz (Fig. 7b).

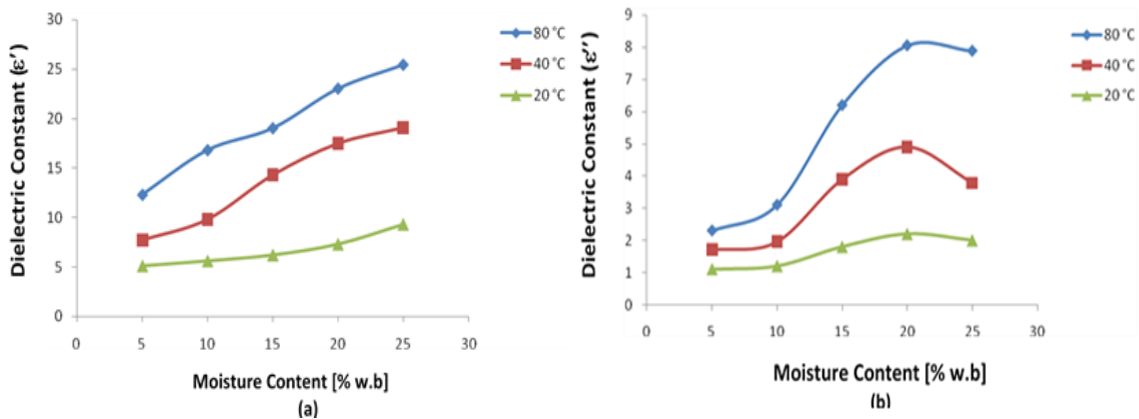


Fig. 7. Variation of the dielectric constant (a) and the loss factor (b) of ZnO@cellulose as a function of the moisture content and different temperatures at 27.12 MHz.

As seen in Table 2, in parallel to the increase of temperature, frequency and moisture content, the penetration depth diminished.

Table 2. Measurement of Dielectric properties (mean  $\pm$  SD of replicates) of ZnO@cellulose at three temperatures and two moisture content levels.

Moisture content	Temperature	$\epsilon'$		$\epsilon''$		Penetration depth (m)		
		13.56 Mhz	27.12 Mhz	13.56 Mhz	27.12 Mhz	13.56 Mhz	27.12 Mhz	
6.9	20 °C	6.79 $\pm$ 0.31	6.46 $\pm$ 0.2	2.30 $\pm$ 0.08	1.2 $\pm$ 0.13	31.1 $\pm$ 0.09	21.6 $\pm$ 0.09	
		6.92 $\pm$ 0.22	6.55 $\pm$ 0.42	4.31 $\pm$ 0.13	3.22 $\pm$ 0.04	21.09 $\pm$ 0.06	15.61 $\pm$ 0.05	
	40 °C	7.97 $\pm$ 0.15	7.57 $\pm$ 0.24	5.43 $\pm$ 0.12	4.99 $\pm$ 0.08	14.9 $\pm$ 0.19	10.51 $\pm$ 0.08	
		80 °C	10.20 $\pm$ 0.3	9.3 $\pm$ 0.13	2.6 $\pm$ 0.17	2.2 $\pm$ 0.09	6.91 $\pm$ 0.22	5.4 $\pm$ 0.1
	14.9	40 °C	21.53 $\pm$ 0.13	19.1 $\pm$ 0.20	5.72 $\pm$ 0.14	4.9 $\pm$ 0.05	3.99 $\pm$ 0.17	0.11 $\pm$ 1.07
		80 °C	27.02 $\pm$ 0.11	25.4 $\pm$ 0.17	9.61 $\pm$ 0.11	8.06 $\pm$ 0.06	2.06 $\pm$ 0.10	0.10

#### 4. Conclusions

In parallel to the increase of the frequency and the compaction density values, the dielectric constant and the loss factor of the ZnO@cellulose decreased, and they increased with increase of the moisture content.

The variation in the dielectric properties of ZnO@cellulose as a function of the variation in the moisture and the temperature was more pronounced at lower frequencies values.

When the compaction density reached a definite level, both the dielectric constant and the loss factor increased with compaction density then decreased. Also, the penetration depth diminished with the moisture content and the temperature of the ZnO@cellulose sample.

#### Acknowledgements

The authors extend their appreciation to the Deanship of Scientific Research at Imam Mohammad Ibn Saud Islamic University for funding this work through Research Group no. RG-21-09-66.

#### References

- [1] Dawei Z, Ying Z, Wanke C, Wenshuai C, Yiqiang W, Haipeng Y., Adv. Mater. 2021;33: 2000619 ; <https://doi.org/10.1002/adma.202000619>
- [2] Holschuh B, Newman D., Smart Mater. Struct. 2015;24:035011 ; <https://doi.org/10.1088/0964-1726/24/3/035011>
- [3] Krupka J, Meas. Sci. Technol. 2006;17:55–70 ; <https://doi.org/10.1088/0957-0233/17/6/R01>
- [4] Leśnikowski J, Tokarska M. Text. Res. J. 2014;84:290-302 ; <https://doi.org/10.1177/0040517513494257>
- [5] Panel JH, Christie SR, Sylvander IM, Woodhead KI. J. Non Cryst. Solids 341 2004;341:115-119 ; <https://doi.org/10.1016/j.jnoncrysol.2004.05.014>
- [6] Sebastián B, Eduardo R, Irati B, Cesar S, Ángel L, Galder. Carbohydr. Polym. 2018;199:20-

- 30 ; <https://doi.org/10.1016/j.carbpol.2018.06.088>
- [7] Emily K, Durham S, Sastry K., *Enzyme Microb. Technol.* 2020;142:109678 ;  
<https://doi.org/10.1016/j.enzmictec.2020.109678>
- [8] Wetterling J, Mattsson T, Theliander H., *Chem. Eng. Sci.* 2017;171:368-378 ;  
<https://doi.org/10.1016/j.ces.2017.05.054>
- [9] Rogier H, *Textile antenna systems: Handbook of Smart Textiles* 2015;433-458 ;  
[https://doi.org/10.1007/978-981-4451-45-1\\_38](https://doi.org/10.1007/978-981-4451-45-1_38)
10. El Ghouli J, Al-Harbi FF., *Solid State Commun.* 2020:113916 ;  
<https://doi.org/10.1016/j.ssc.2020.113916>
- [11] Halliday D, Resnick R, Walker J. *Fundamentals of Physics*, sixth ed. Wiley, New York 2001.
- [12] Buffler GR. *Microwave cooking and processing.* Van nostrand reinhold. New York 1993 ;  
<https://doi.org/10.1007/978-1-4757-5833-7>
- [13] Guan D, Cheng M, Wang Y, Tang J, *J. Food Sci.* 2004;69:30-37 ;  
<https://doi.org/10.1111/j.1365-2621.2004.tb17864.x>
- [14] Halliday D, Resnick R, Walker J., *Fundamentals of Physics*, sixth ed. Wiley, New York 2001.
- [15] Thawatchai M, Seiichi R, Tokura R., *Carbohydr. Polym.* 2008 ;72:43-51.  
<https://doi.org/10.1016/j.carbpol.2007.07.025>
16. Ananthu C.M, Renjanadevi B., *Procedia Technology* 2016;24:761-766 ;  
<https://doi.org/10.1016/j.protcy.2016.05.078>
17. Khoshhesab ZM, Sarfaraz M, Asadabad MA., *Metal-Organic and Nano-Metal Chemistry* 2011;41:814-819 ; <https://doi.org/10.1080/15533174.2011.591308>
18. JCPDS, Powder Diffraction File, Alphabetical Index, Inorganic Compounds, International Centre for Diffraction Data, Newtown Square, Pa, USA, 1977.
19. Siqueira G, Bras J, Dufresne A. *Polymers* 2010;2:728-765 ;  
<https://doi.org/10.3390/polym2040728>